Crystallographic and EXAFS Studies of Conformationally Designed Nonplanar Nickel(II) Porphyrins

Kathleen M. Barkigia,[1a] Mark W. Renner,[1a] Lars R. Furenlid,[1a,b] Craig J. Medforth,[1c] Kevin M. Smith,[1c] and Jack Fajer*,[1a]

Contribution from the Department of Applied Science and National Synchrotron Light Source, Brookhaven National Laboratory, Upton, New York 11973, and Department of Chemistry, University of California, Davis, California 95616

Received December 29, 1992

Abstract: A series of Ni(II) tetraphenylporphyrins with varying β substituents was examined by X-ray crystallography and EXAFS to assess peripheral steric effects on the conformations of the macrocycles. The compounds are the low-spin Ni(II) derivatives of 2,3,7,8,12,13,17,18-octaethyl-5,10,15,20-tetraphenylporphyrin (**1**), 2,3,7,8,12,13,17,-18-octapropyl-5,10,15,20-tetraphenylporphyrin (**2**), 2,3,7,8,12,13,17,18-tetracyclohexenyl-5,10,15,20-tetraphenylporphyrin (**3**), 2,3,5,7,8,10,12,13,15,17,18,20-dodecaphenylporphyrin (**4**), 2,3,7,8,12,13,17,18-tetracyclopentenyl-5,10,15,20-tetraphenylporphyrin (**5**), and 2,3,7,8,12,13,17,18-tetracyclopentenyl-5,10,15,20-tetrakis(3,4,5-trimethoxyphenyl)porphyrin (**6**). X-ray structures of **1**, **2**, and **3** reveal that the molecules are severely nonplanar and assume saddle shapes in which the pyrrole rings lie alternately above and below the porphyrin planes with β carbon displacements of more than 1 Å while the meso carbons remain in plane. **1** crystallizes with three methanols of solvation per porphyrin that form an unusual infinite hydrogen-bonded methanol network that transverses one axis of the crystal. Advantage is taken of the fact that short and long Ni–N distances are diagnostic of ruffled and planar Ni macrocycles, respectively, to establish the conformations of the molecules in solution and in the amorphous state by EXAFS. Within the precision of the EXAFS data (0.02 Å), the Ni–N distances in **1**, **2**, and **3** are the same in solution and in amorphous powders as in the crystals and establish therefore that the distorted conformations of the compounds are maintained in all three phases. EXAFS data for **4**, whose structure is unknown, indicate an equally distorted geometry in solution and in the powder. In contrast to **1**–**4**, EXAFS results for **5** and **6** as powders, and for **6** in solution, clearly signal planar conformations for the two tetracyclopentenyl derivatives. Further evidence that **6** is not sterically constrained derives from the observation that it can be converted to a high-spin hexacoordinated Ni(II) complex in pyridine (**5** is insoluble). The conformations and Ni–N distances obtained crystallographically or by EXAFS for **1**–**6** agree well with previous molecular mechanics calculations. The macrocycle distortions induce optical red shifts attributed to a smaller gap between the HOMOs and LUMOs of the porphyrins. In particular, the first optical transition, which is principally a HOMO to LUMO excitation, is correctly predicted by INDO/s calculations based on the crystal coordinates for **1**, **2**, and **3** reported here. An additional assessment of the effects of the substituents and macrocycle conformations on the frontier orbitals of the molecules is obtained from cyclic voltammetry measurements of oxidation and reduction potentials which provide an experimental probe of the migration of the HOMOs and LUMOs; the electrochemically determined differences in redox potentials mirror the first optical transitions. Crystallographic data: $NiN_4C_{60}H_{60}\cdot 3CH_3OH$ (**1**): triclinic space group $P\bar{1}$, $a = 13.739(1)$ Å, $b = 17.055(4)$ Å, $c = 12.938(2)$ Å, $\alpha = 96.89(1)°$, $\beta = 107.66(1)°$, $\gamma = 104.58(2)°$, $V = 2731.7$ Å^3, $Z = 2$, $R_F = 0.066$ and $R_{wF} = 0.091$ based on 8077 reflections with $F_o > 6\sigma F_o$. $NiN_4C_{68}H_{76}$ (**2**): monoclinic space group $P2_1/n$, $a = 15.195(8)$ Å, $b = 19.577(9)$ Å, $c = 19.137(5)$ Å, $\beta = 98.77(3)°$, $V = 5626.2$ Å^3, $Z = 4$, $R_F = 0.054$ and $R_{wF} = 0.060$ based on 5716 reflections with $F_o > 3\sigma F_o$. $NiN_4C_{60}H_{52}\cdot CH_2Cl_2$ (**3**): tetragonal space group $I\bar{4}$, $a = b = 32.111(11)$ Å, $c = 9.876(8)$ Å, $V = 10183$ Å^3, $Z = 8$, $R_F = 0.081$ and $R_{wF} = 0.108$ based on 3161 reflections with $F_o > 2\sigma F_o$. $T = 200$ K.

Introduction

An expanding body of structural data for porphyrins, chlorins, bacteriochlorins, and isobacteriochlorins as isolated molecules and in proteins illustrates the considerable flexibility of the molecules, and the significant distortions that can be imposed on porphinoid macrocycles by crystal packing, steric effects, or protein constraints.[2-9] Recent theoretical and experimental studies have documented the consequences of such conformational variations on the optical, redox, EPR, NMR, vibrational, excited state, and electron-transfer properties of porphyrin derivatives.[9-16] Interest in these structural effects is prompted by the ubiquitous and multifaceted roles of porphyrins in bioenergetics ranging from photosynthesis, methanogenesis, nitrite and sulfite reduction to vitamin B_{12} and heme chemistry in vivo, and the considerable effort now devoted to biomimetic solar energy conversion and catalysis, photodynamic therapy as well as basic mechanisms of electron transfer.[2-20]

Several recent crystallographic studies[9-13,17,18] have led to the concept of "conformationally designed" porphyrins whereby the introduction of multiple substituents on the periphery of porphyrins induces large deformations of the macrocycles that minimize steric interactions between the substituents. Although NMR and resonance Raman results as well as the altered

(1) (a) Department of Applied Science. (b) National Synchrotron Light Source, Brookhaven National Laboratory. (c) University of California.

(2) Scheidt, W. R.; Lee, Y. J. *Struct. Bonding (Berlin)* **1987**, *64*, 1.
(3) Barkigia, K. M.; Fajer, J. In *The Photosynthetic Reaction Center*; Deisenhofer, J., Norris, J. R., Eds.; Academic Press: San Diego, 1993; Vol. II, p 513.
(4) Kratky, C.; Waditschatka, R.; Angst, C.; Johansen, J. E.; Plaquevent, J. C.; Schreiberg, J.; Eschenmoser, A. *Helv. Chim. Acta* **1985**, *68*, 1312. Barkigia, K. M.; Fajer, J.; Chang, C. K.; Williams, G. J. B. *J. Am. Chem. Soc.* **1982**, *104*, 315. Suh, M. P.; Swepston, P. M.; Ibers, J. A. *J. Am. Chem. Soc.* **1984**, *106*, 5164. Strauss, S. H.; Silver, M. E.; Long, K. M.; Thompson, R. G.; Hudgens, R. A.; Spartalian, K.; Ibers, J. A. *J. Am. Chem. Soc.* **1985**, *107*, 4207. Stolzenberg, A. M.; Glazer, P. A.; Foxmann, B. M. *Inorg. Chem.* **1986**, *25*, 983. Brennan, T. D.; Scheidt, W. R.; Shelnutt, J. A. *J. Am. Chem. Soc.* **1988**, *110*, 3919.

0002-7863/93/1515-3627$04.00/0

properties of the distorted molecules[9-13,17,18] certainly suggest that the nonplanar conformations found in single crystals are conserved in solution, a basic question to be answered is how faithfully these distortions are maintained in solution since most porphyrin chemistry is carried out in solution (or in proteins) and not in the solid state. We address this question by taking advantage of extended X-ray absorption fine structure (EXAFS) techniques that yield metal–nitrogen distances with a reliability of ~0.02 Å (based on previous studies[14]) and thus allow direct comparison with crystallographic results. Furthermore, in the case of Ni(II) porphyrins, hydroporphyrins, and porphycenes, Ni–N bond lengths have proved to be accurate reporters of the conformations of the macrocycles: short Ni–N distances are diagnostic of nonplanar macrocycles, whereas long distances are typical of planar molecules.[2,4,11,12,14,17-20] We present here solution EXAFS and crystallographic results for three peripherally crowded Ni(II) porphyrins, 2,3,7,8,12,13,17,18-octaethyl-5,10,-15,20-tetraphenylporphyrin (OETPP, **1**), 2,3,7,8,12,13,17,18-octapropyl-5,10,15,20-tetraphenylporphyrin (OPrTPP, **2**), and 2,3,7,8,12,13,17,18-tetracyclohexenyl-5,10,15,20-tetraphenylporphyrin (TC_6TPP, **3**), see Figure 1. The two techniques yield similar Ni–N distances and establish therefore that the crystallographic conformations are maintained in solution. Thus, the physical and chemical properties measured in solution do indeed reflect the stereochemistry of the single crystals. In addition, EXAFS data for the Ni complexes of 2,3,5,7,8,10,-12,13,15,17,18,20-dodecaphenylporphyrin (DPP, **4**) and 2,3,7,8,-12,13,17,18-tetracyclopentenyl-5,10,15,20-tetraphenylporphyrin (TC_5TPP, **5**), which could not be crystallized, indicate that the former is nonplanar while the latter is planar.

As well, solution and powder EXAFS data for the Ni(II) complex of 2,3,7,8,12,13,17,18-tetracyclopentenyl-5,10,15,20-tetrakis(3,4,5-trimethoxyphenyl)porphyrin ($TC_5T(OMeP)P$, **6**) also indicate a planar conformation in agreement with molecular mechanics calculations and solution NMR results but in contrast to crystallographic data that reveal a slightly ruffled conformation.[12c]

As has been observed for other distorted porphyrins, **1–4** exhibit red-shifted optical absorption spectra which are correctly predicted by semiempirical INDO/s calculations.[9-12] An additional assessment of the effects of the macrocycle distortions on the highest occupied (HOMO) and lowest unoccupied (LUMO) molecular orbitals is obtained from cyclic voltammetry measurements of the first oxidation and reduction potentials which provide an experimental probe of the migration of the frontier orbitals of the compounds.

Methods

The syntheses of compounds **1–6** have been reported.[11,12] Ni(II) 5,10,15,20-tetrakis(3,4,5-trimethoxyphenyl)porphyrin (NiT(OMeP)P, **7**) was prepared by condensation of 3,4,5-trimethoxybenzaldehyde with pyrrole followed by insertion of Ni using the acetate method[10,12b,c] (λ_{max} in CH_2Cl_2: 418, 527, and 549 (sh) nm). Optical spectra were recorded on Cary 2300 or Hewlett Packard 8452A diode array spectrophotometers. Redox potentials were determined by cyclic voltammetry in butyronitrile with 0.1 M Bu_4NClO_4 as supporting electrolyte on a BAS100A electrochemical analyzer. Solvents were dried and distilled immediately before use. Optical spectra were calculated with the INDO/s (intermediate neglect of differential overlap) method developed by Zerner and co-workers[21] for optical spectra of porphyrins. The method consists of a ground-state self-consistent field calculation followed by monoexcited configuration interaction. Excitations were generated from an active space comprised of 11 HOMOs and 11 LUMOs. The coordinates reported here were used in the calculations.

EXAFS spectra were obtained on beam lines X-11A and X-19A at the Brookhaven National Synchrotron Light Source. Ni(II) samples were prepared as either fine powders or as ~2 mM toluene solutions (tetrahydrofuran in the case of **3**) in 3-mm thick glass cells with thin aluminized Mylar windows (2 mil).[14] Samples were measured in fluorescence mode at room temperature and also at 110 K for **6**. EXAFS oscillations were isolated using standard techniques as reported recently.[14] Quantitative analyses were performed with experimental standards[14] and with FEFF, an ab initio curved-wave EXAFS simulation code.[22] First shell EXAFS spectra were simulated for Ni coordinated by four nitrogens using default input parameters. The FEFF method was calibrated against Ni(II) tetrapropylporphycene. The average Ni–N distances of 1.896(2) Å from the crystal structure[23] agree well with the value of 1.89(2) Å derived from FEFF with

(5) Chow, H. C.; Serlin, R.; Strouse, C. E. *J. Am. Chem. Soc.* **1975**, *97*, 7230. Serlin, R.; Chow, H. C.; Strouse, C. E. *J. Am. Chem. Soc.* **1975**, *97*, 7237. Kratky, C.; Dunitz, J. D. *Acta Crystallogr., Sect. B* **1975**, *B32*, 1586; **1977**, *B33*, 545. Kratky, C.; Dunitz, J. D. *J. Mol. Biol.* **1977**, *113*, 431. Kratky, C.; Isenring, H. P.; Dunitz, J. D. *Acta Crystallogr., Sect. B* **1977**, *B33*, 547. Smith, K. M.; Goff, D. A.; Fajer, J.; Barkigia, K. M. *J. Am. Chem. Soc.* **1982**, *104*, 3747; **1983**, *105*, 1674. Fajer, J.; Barkigia, K. M.; Fujita, E.; Goff, D. A.; Hanson, L. K.; Head, J. D.; Horning, T.; Smith, K. M.; Zerner, M. C. In *Antennas and Reaction Centers of Photosynthetic Bacteria*; Michel-Beyerle, M. D., Ed.; Springer-Verlag: Berlin, 1985; p 324.

(6) Barkigia, K. M.; Fajer, J.; Chang, C. K.; Young, R. *J. Am. Chem. Soc.* **1984**, *106*, 6457. Waditschatka, R.; Kratky, C.; Jaun, B.; Heinzer, J.; Eschenmoser, A. *J. Chem. Soc., Chem. Commun.* **1985**, 1604. Barkigia, K. M.; Gottfried, D. S.; Boxer, S. G.; Fajer, J. *J. Am. Chem. Soc.* **1989**, *111*, 6444.

(7) Deisenhofer, J.; Michel, H. *Science* **1989**, *245*, 1463, and references therein.

(8) Tronrud, D. E.; Schmid, M. F.; Matthews, B. W. *J. Mol. Biol.* **1986**, *188*, 443.

(9) Barkigia, K. M.; Chantranupong, L.; Smith, K. M.; Fajer, J. *J. Am. Chem. Soc.* **1988**, *110*, 7566.

(10) Barkigia, K. M.; Berber, M. D.; Fajer, J.; Medforth, C. J.; Renner, M. W.; Smith, K. M. *J. Am. Chem. Soc.* **1990**, *112*, 8851.

(11) (a) Medforth, C. J.; Berber, M. D.; Smith, K. M.; Shelnutt, J. A. *Tetrahedron Lett.* **1990**, *31*, 3719. (b) Shelnutt, J. A.; Medforth, C. J.; Berber, M. D.; Barkigia, K. M.; Smith, K. M. *J. Am. Chem. Soc.* **1991**, *113*, 4077.

(12) (a) Sparks, L. D.; Medforth, C. J.; Park, M. S.; Chamberlain, J. R.; Ondrias, M. R.; Senge, M. O.; Smith, K. M.; Shelnutt, J. A. *J. Am. Chem. Soc.* **1993**, *115*, 581. (b) Medforth, C. J.; Senge, M. O.; Smith, K. M.; Sparks, L. D.; Shelnutt, J. A. *J. Am. Chem. Soc.* **1992**, *114*, 9859. (c) Senge, M. O.; Medforth, C. J.; Sparks, L. D.; Shelnutt, J. A.; Smith, K. M. *Inorg. Chem.*, in press.

(13) Renner, M. W.; Cheng, R.-J.; Chang, C. K.; Fajer, J. *J. Phys. Chem.* **1990**, *94*, 8508. Forman, A.; Renner, M. W.; Fujita, E.; Barkigia, K. M.; Evans, M. W.; Smith, K. M.; Fajer, J. *Isr. J. Chem.* **1989**, *29*, 57.

(14) Furenlid, L. R.; Renner, M. W.; Smith, K. M.; Fajer, J. *J. Am. Chem. Soc.* **1990**, *112*, 1634. Furenlid, L. R.; Renner, M. W.; Fajer, J. *J. Am. Chem. Soc.* **1990**, *112*, 8987. Renner, M. W.; Furenlid, L. R.; Barkigia, K. M.; Forman, A.; Shim, H. K.; Simpson, D. J.; Smith, K. M.; Fajer, J. *J. Am. Chem. Soc.* **1991**, *113*, 6891.

(15) Gudowska-Nowak, E.; Newton, M. D.; Fajer, J. *J. Phys. Chem.* **1990**, *94*, 5795. Barkigia, K. M.; Thompson, M. A.; Fajer, J.; Pandey, R. K.; Smith, K. M.; Vicente, M. G. H. *New J. Chem.* **1992**, *16*, 599. Fajer, J.; Barkigia, K. M.; Smith, K. M.; Zhong, E.; Gudowska-Nowak, E.; Newton, M. In *Reaction Centers of Photosynthetic Bacteria*; Michel-Beyerle, Ed.; Springer-Verlag: Berlin, 1990; p 367.

(16) Fajer, J. *Chem. Ind.* **1991**, 869 and references therein.

(17) Mandon, D.; Ochsenbein, P.; Fischer, J.; Weiss, R.; Jayaraj, K.; Austin, R. N.; Gold, A.; White P. S.; Brigaud, O.; Battioni, P.; Mansuy, D. *Inorg. Chem.* **1992**, *31*, 2044.

(18) Lyons, J. E.; Ellis, P. E.; Wagner, R. W.; Thompson, P. B.; Gray, H. B.; Hughes, M. D.; Hodge, J. A. Preprints; Division of Petroleum Chemistry; American Chemical Society: San Francisco, CA, 1992; Vol. 37, p 307. Henling, L. M.; Schaefer, W. P.; Hodge, J. A.; Hughes, M. E.; Gray, H. B.; Lyons, J. E.; Ellis, P. E. *Acta Crystallogr.*, in press. Schaefer, W. P.; Hodge, J. A.; Hughes, M. E.; Gray, H. B.; Lyons, J. E.; Ellis, P. E.; Wagner, R. W. *Acta Crystallogr.*, in press.

(19) Fäber, G.; Keller, W.; Kratky, C.; Jaun, B.; Pfaltz, A.; Spinner, C.; Kobelt, A.; Eschenmoser, A. *Helv. Chim. Acta* **1991**, *74*, 697.

(20) For additional examples, see the following: *The Bioinorganic Chemistry of Nickel*; Lancaster, J. R., Ed.; VCH Publishers: New York, 1988. (a) Eidsness, M. K.; Sullivan, R. J.; Scott, R. A. p 73. Wackett, L. P.; Honek, J. F.; Begley, T. P.; Shames, S. L.; Niederhoffer, E. C.; Hausinger, R. P.; Orme-Johnson, W. H.; Walsh, C. T. p 249. Pfaltz, A. p 275.

(21) Ridley, J.; Zerner, M. *Theor. Chim. Acta (Berlin)* **1973**, *32*, 111; **1976**, *42*, 223. Zerner, M.; Loew, G.; Kirchner, R.; Mueller-Westerhoff, U. *J. Am. Chem. Soc.* **1980**, *102*, 589.

(22) Rehr, J. J.; Mustre de Leon, J.; Zabinsky, S. I.; Albers, R. C. *J. Am. Chem. Soc.* **1991**, *113*, 5135. Mustre de Leon, J.; Rehr, J. J.; Zabinsky, S. I. *Phys. Rev. B* **1991**, *44*, 4146.

(23) Vogel, E.; Balci, M.; Pramod, K.; Koch, P.; Lex, J.; Ermer, O. *Angew. Chem., Int. Ed. Engl.* **1987**, *26*, 928.

Table I. Experimental Crystallographic Details for 1, 2, and 3

	1	2	3
crystallized from	MeOH/$CHCl_3$	CH_2Cl_2/MeOH	CH_2Cl_2/MeOH
formula	$NiN_4C_{60}H_{60}\cdot 3CH_3OH$	$NiN_4C_{68}H_{76}$	$NiN_4C_{60}H_{52}\cdot CH_2Cl_2$
mw	992.0	1008.1	972.8
space group	$P\bar{1}$	$P2_1/n$	$I\bar{4}$
a, Å	13.739(1)	15.195(8)	32.111(11)
b, Å	17.055(4)	19.577(9)	32.111(11)
c, Å	12.938(2)	19.137(5)	9.876(8)
α, °	96.89(1)	80.0	90.0
β, °	107.66(1)	98.77(3)	90.0
γ, °	104.58(2)	90.0	90.0
V, Å^3	2731.7	5626.2	10183
Z	2	4	8
crystal size, mm	0.42 × 0.22 × 0.26	0.32 × 0.11 × 0.24	0.30 × 0.11 × 0.11
data collection	CAD4	CAD4	CAD4
λ, Å	1.5418	1.5418	1.5418
scan	θ–2θ	θ–2θ	θ–2θ
2θ range, deg	4–150	4–120	4–120
data measd	$h\pm k\pm l$, some $\bar{h}\bar{k}l$	$hk\pm l$, some $\bar{h}k\pm l$	hkl, excluding body centering
no. measd	13327	11847	4650
unique	11226	8616	4160
R_{av}	0.017	0.031	0.022
u, cm^{-1}	8.531	7.960	18.43
absorptn correctn	analytical	analytical	analytical
transmission coeff	0.7386–0.8580	0.7893–0.9183	0.7587–0.8467
refinement	8077 data with $F_o > 6\sigma F_o$	5716 with $F_o > 3\sigma F_o$	3161 with $F_o > 2\sigma F_o$
R_F	0.066	0.054	0.081
R_{wF}	0.091	0.060	0.108
T, K	200	200	200

minor E_o (3.0 eV) adjustments. Additional details of the analyses are included in the supplementary material.

Crystallography. Crystals of compounds **1**, **2**, and **3** were mounted on glass fibers and examined at room temperature. Full data sets were collected for all three on an Enraf-Nonius CAD4 diffractometer. Subsequently, the crystals were cooled to 200 K, using an Enraf-Nonius FR558-S cooling system, and the data sets were remeasured. All the results reported here are based on the 200K data. (See Table I for experimental details.)

Lattice parameters were determined using 25 reflections measured at $\pm 2\theta$ for all samples. Three standard reflections were checked periodically to monitor crystal movement and possible decay. Based on analysis of these standard reflections, no decay correction was deemed necessary. Data were treated for Lorentz, polarization, and absorption using the CRYSNET[24] series of programs.

The structures of **1** and **2** were solved using the direct methods option of SHELXS-86.[25] The structure of **3** was extracted from a Patterson solution produced by SHELXS-86, in space group $I\bar{4}$. (Since space group $I\bar{4}$ is not uniquely determined, solutions were also attempted in $I4/m$ and $I4$.) The structural models of the three compounds were completed using difference Fourier techniques.

All three structures were refined using full-matrix least-squares, allowing all non-hydrogen atoms anisotropic expression of their thermal motion, until convergence was reached. Hydrogens were included in idealized positions (C–H = 0.95 Å) with fixed isotropic thermal parameters. Scattering factors were taken from standard compilations,[26] and the anomalous terms for Ni were included in all three refinements. (For **3**, anomalous terms for the chlorines of the CH_2Cl_2 of crystallization were also included.)

(24) Informal Report BNL #21714; Berman, H. M., Bernstein, F. C., Bernstein, H. J., Koetzle, T. F., Williams, G. J. B., Eds.; Brookhaven National Laboratory: Upton, NY, 1976.

(25) Sheldrick, G. M. *Crystallographic Computing 3*; Sheldrick, G. M., Kruger, C., Goddard, R., Eds.; Oxford University Press: 1985; p 175.

(26) Scattering factors for non-hydrogen atoms were taken: Cromer, D. T.; Mann, J. B. *Acta Crystallogr., Sect. A* **1968**, *A24*, 321. Scattering factors for hydrogens: Stewart, R. F.; Davidson, E. R.; Simpson, W. T. *J. Chem. Phys.* **1965**, *42*, 3175. The anomalous components are taken: *International Tables for X-ray Crystallography*; Kynoch Press: Birmingham, England, 1974; Vol. IV, p 148.

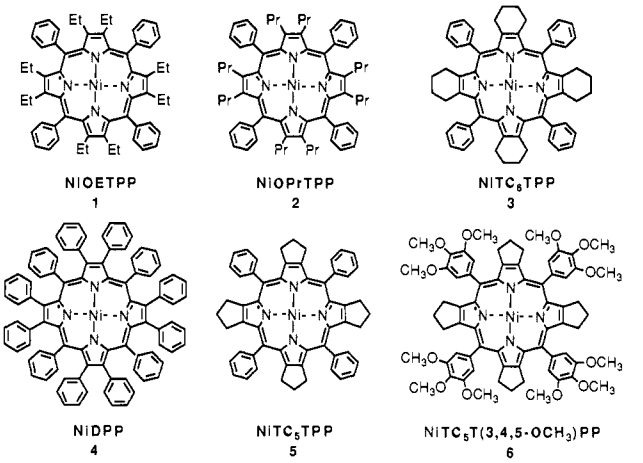

Figure 1. Structural formulas of NiOETPP (**1**), NiOPrTPP (**2**), NiTC$_6$TPP (**3**), NiDPP (**4**), NiTC$_5$TPP (**5**), and NiTC$_5$T(OMeP)P (**6**).

For compound **3**, in order to correctly account for the equivalent reflections in the noncentrosymmetric point group $\bar{4}$, the averaging was redone, and both senses of the indices were refined. The results of the refinement which produced the lower R values are presented here. Positional and thermal parameters for **1**, **2**, and **3** are given in the supplementary material.

Crystals of **2** undergo a reversible phase transition from space group $C2/c$ to $P2_1/n$, upon cooling from room temperature to 200 K. All derived parameters, including conformational details, are very similar at the two temperatures. Details of the room temperature analysis are given in the supplementary material.

Results and Discussion

Crystallography. The molecular structures of **1**, **2**, and **3** are presented in Figure 2. Bond distances in **1**, which are typical for the series, are given in Figure 3. Data for **2** and **3** are included in the supplementary material. The molecules are severely nonplanar and adapt S_4 saddle[27] conformations as is evident from Figure 4 which presents the displacements of the skeletal atoms from the planes defined by the four nitrogens and by the 24 core atoms of the macrocycles.

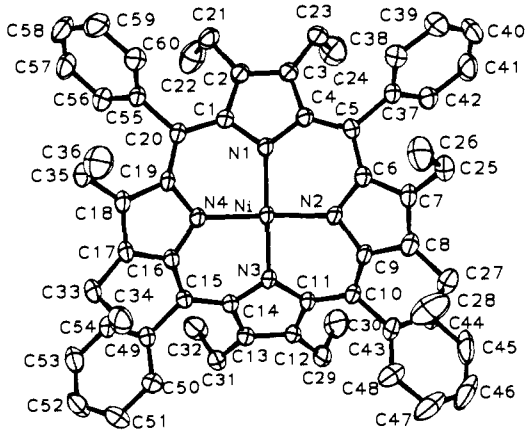

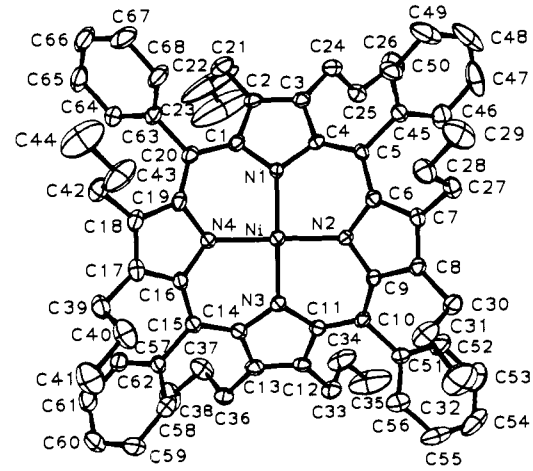

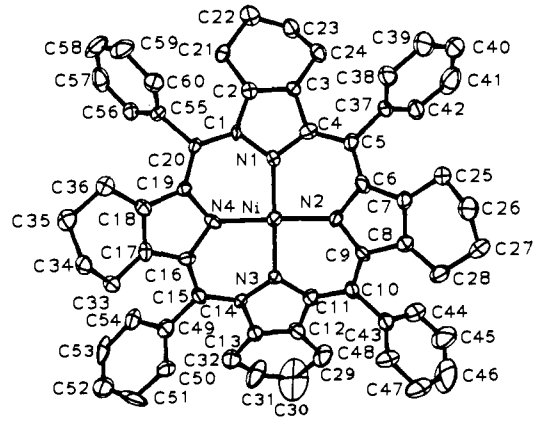

Figure 2. Molecular structures of **1** (top), **2** (middle), and **3** (bottom). Thermal ellipsoids enclose 50% probability. Hydrogens are omitted for clarity.

2 is the most distorted of the three compounds. The average displacement of the Cβ atoms from the mean plane of the molecule is 1.28(2) Å. This diminishes to 1.23(1) Å in **1** and 1.08(1) Å in **3**. As anticipated for a saddle conformation,[2] the meso carbons (Cm) lie nearly in the planes of the macrocycles. Since the saddle is steepest in **2**, the angles between adjacent and opposite pyrrole rings are also the largest. For adjacent rings, they average 42.3°, 40.1°, and 34.5° for **2**, **1**, and **3**, respectively, and for opposite rings, 61.2°, 58.0°, and 49.6°. Individually, each pyrrole ring in the three structures is planar with the largest deviations from the mean pyrrole planes at the nitrogens. Further evidence of the planarity of the pyrroles derives from the small CαCβCβCα dihedral angles whose values range from 0.2 to 1.4°. Additional structural parameters for these and related compounds are presented in Table II.

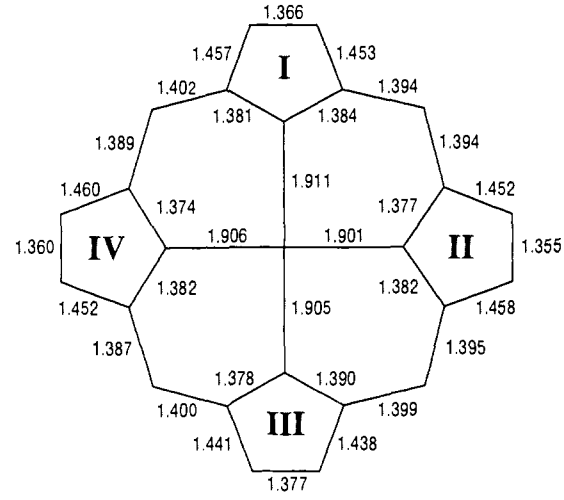

Figure 3. Bond distances in **1** (Å). The esd's are 0.005 Å for a typical C–C bond and 0.003 Å for the Ni–N distances.

As is commonly found in tetraarylporphyrins with saddle conformations,[2,10-13,17,18] the phenyl rings rotate into the porphyrin planes to minimize unfavorable contacts with the β substituents. The average dihedral angles of the phenyl rings with the macrocycle planes are 39(3)°, 43(1)°, and 50(2)° in **2**, **1**, and **3**, respectively, and thus correlate with the degree of distortion of the molecules; the steeper saddles result in more acute dihedral angles for the phenyl rings. This trend is maintained in all the peripherally crowded saddle porphyrins reported to date.[10-13,17,18] In spite of the increased rotations of the phenyl rings, the bonds between the meso carbons and the phenyl rings are clearly single bonds with average values of 1.491(1), 1.493(3), and 1.488(6) Å in **1**, **2**, and **3**, respectively, and do not indicate any shortening suggestive of increased conjugation between the porphyrin and phenyl rings.

Saddle conformations presumably minimize unfavorable contacts between meso and β substituents.[2] Indeed, the average distances between the ortho carbons of the phenyl rings and the Cβ atoms of the pyrroles are long: 3.40(2) Å in **1** and **3** and 3.38(2) Å in **2**. The separation between the *o*-phenyl carbons and the methylene carbons of the substituents on the β pyrrole positions are also long and average 3.36(2), 3.34(2) and 3.33(3) Å in **1**, **2**, and **3**, respectively.

Since the pyrrole rings swivel alternately up and down about the meso carbons which remain essentially in plane (see Figure 4), those angles are obviously most affected by the saddle conformations. The values of the CβCαCm angles average 127.1(3)°, 128.3(1)°, and 129.1(1)° in **3**, **1**, and **2**, respectively, and thus correlate with increasing distortion of the saddle. All these angles are larger than those calculated for Hoard's "average" porphyrin:[28] 124.2(1)°. In contrast, the NCαCm angles become more acute with increasing distortions, 122.3(3)°, 121.3(2)°, and

(27) Two distinct geometries are commonly found in ruffled porphyrins. One is the saddle conformation exhibited by **1**, **2**, and **3** here in which the pyrrole rings are displaced alternately above and below the mean plane of the core, and the meso carbons remain in or nearly in plane. The other geometry is one in which the pyrrole ring twists so that the β carbons lie above and below the core plane as do the meso carbons. The two conformations have been labeled *sad* and *ruf* by Scheidt and Lee.[2] For simplicity, we use "saddle" for the *sad* conformation discussed here, and *ruf* when it is specifically required to distinguish between the two.

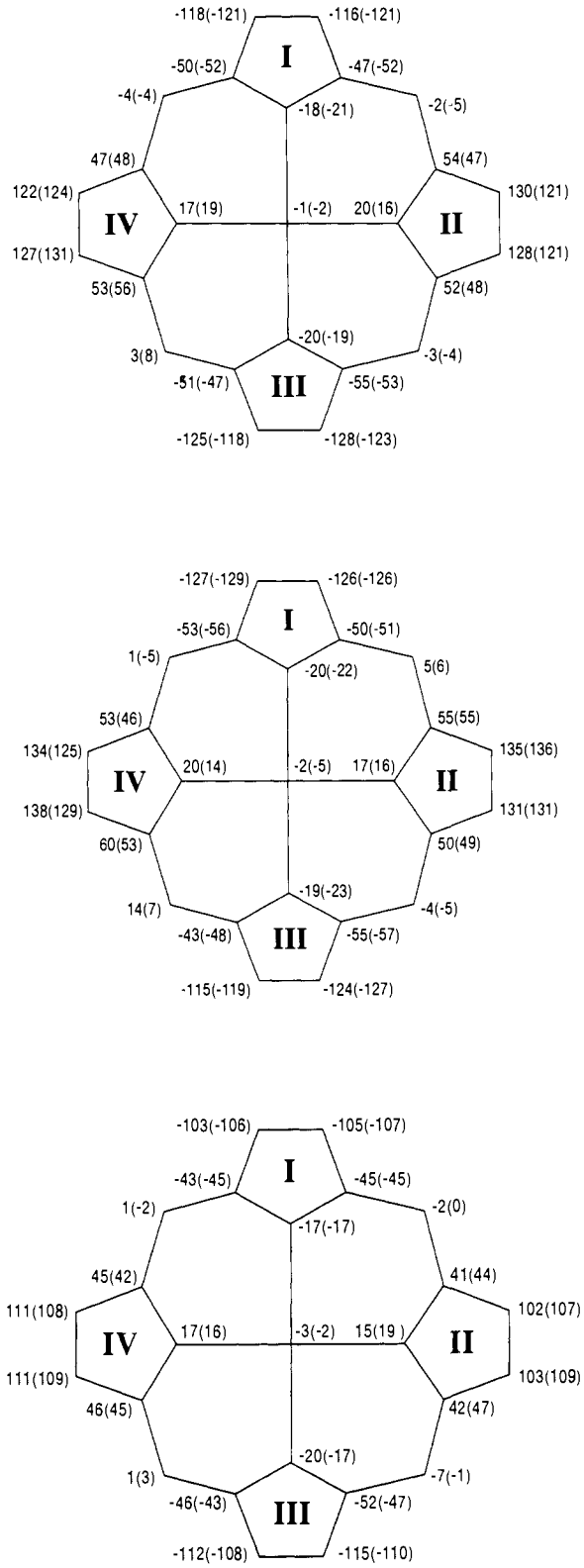

Figure 4. Displacements of the 24 atoms that comprise the porphyrin cores of **1** (top), **2** (middle), and **3** (bottom) from the planes defined by the four nitrogens and, in parentheses, from the mean planes of the 24 atoms, in units of 0.01 Å.

120.8(1)° for **3**, **1**, and **2**, and are all smaller than the Hoard average of 125.7(2)°. The CαCmCα angles are essentially invariant in the series, 121.4(1)°, 121.5(2)°, and 121.8(5)° for **1**, **2**, and **3**, but are smaller than the Hoard average, 123.8(3)°. The NCαCβ angles are unaffected in the series, 109.8(1)°, 109.5-(1)° and 110.0(2)°, and are comparable to the value of 110.2-(3)° in Hoard's average. Similarly, the CαNCα angles are constant in the present series, 105.9(2)°, 105.8(1) and 105.6(5)° in **1**, **2**, and **3**, and unperturbed from Hoard's average of 105.5-(3)°. The latter values are sensitive to the metal in the OETPP series,[12a] however, and increase to 107.7(5)° for the Zn complex.[10]

As in ZnOETPP,[10] the ethyl and propyl groups of **1** and **2** are symmetrically arranged up and down on adjacent rings. The cyclohexenyl rings of **3** follow the same pattern, but the thermal motion of the exterior carbons of the rings is high, their conformations are not rigid, and their overall shapes vary (Figure 5).

Each molecule of **3** has a CH_2Cl_2 of solvation associated with it. The CH_2Cl_2 is well-ordered and is tucked into the crevice between opposite cyclohexenyl rings (Figure 5). The distance between the carbon of the solvent molecule and the Ni atom is 3.53 Å. The combination of saddle shapes and up and down orientations of the β substituents in these sterically encumbered molecules may thus form a natural pocket for substrates that may enhance the catalytic activity of the porphyrins.[12,17]

The lattice of **1** contains three methanol molecules of solvation per porphyrin. Although their thermal motion is high, they clearly form novel infinite hydrogen-bonded chains wrapping around the crystallographic *c*-axis. The methanols do *not* interact with the Ni center but instead are located outside pairs of the porphyrins, as illustrated in Figure 6. Oxygen O2 of methanol 2 hydrogen bonds to O1 of methanol 1 with an O···O contact of 2.77 Å and to O3 of methanol 3 with an O···O distance of 2.61 Å. O1 further hydrogen bonds across a center of symmetry to another O1 at an O···O distance of 2.56 Å. Likewise, O3 hydrogen bonds to another O3 across a center of symmetry with O···O contacts of 2.55 Å.

The multiple substituents on **1**, **2**, and **3** preclude the possibility that strong π–π interactions induce the saddle distortions as found in tetraarylporphyrin π cation radicals.[2] There are no intermolecular distances between pyrrole ring centers less than 5 Å, and the vertical separations between the mean planes of the molecules are large, 6.51, 7.11, and 6.18 Å, as are the center-to-center distances, 8.02, 8.90, and 9.88 Å, in **1**, **2**, and **3**, respectively. The molecules of **1** and **2** are related by centers of symmetry and thus exist as loose dimers, whereas the nearest neighbors of **3** arise from translationally related molecules along the *c*-axis.

In all three structures, the Ni atoms are tetracoordinated by the pyrrole nitrogens only. The Ni–N distances are short and are marginally shortest, 1.902(2) Å in **2**, the most distorted molecule, and lengthen to 1.906(2) Å in **1** and to 1.914(9) Å in **3**. For comparison, in the similarly saddled and sterically crowded β halogenated derivatives, the Ni–N distances average 1.896(10) and 1.903(1) Å in two independent determinations of NiTPFOBP[17,18] and 1.916(12) Å in NiTMOBP.[17] In contrast, the Ni–N distances in several planar porphyrins substituted at either the β or meso positions are typically equal or greater than 1.95 Å.[28] The clear correlation between the conformations of the molecules and the short or long Ni–N distances is also maintained in the more saturated hydroporphyrins.[4,14,19,20]

X-ray Absorption: EXAFS and Near-Edge Structure. The correlation of Ni–N distances with the conformations of Ni(II) porphyrins suggests that EXAFS data should provide a useful probe of the conformations of Ni macrocycles in solution. In addition, the X-ray absorption edges of nickel complexes have been shown to be highly sensitive to the coordination geometry around the metal. In square-planar complexes, a distinct peak, attributed to a $1s \rightarrow 4p_z$ electronic transition, is present at approximately 6 eV below the main absorption edge. Introduction of one or two axial ligands results in the attenuation of the preedge peak.[14,20a] Edge studies thus serve as convenient probes of the coordination geometry of Ni complexes.

(28) Hoard, J. L. In *Porphyrins and Metalloporphyrins*; Smith, K. M., Ed.; Elsevier: Amsterdam, 1975; p 317.

Table II. Comparison of Selected Bond Distances (Å) and Angles (deg)[a]

	NiOETPP (*1*)	NiOPrTPP (*2*)	NiTC$_6$TPP (*3*)	NiTMOBP[b]	NiTPFPOBP[c]	NiOEP[d]	"average"[e]
			Bond Distances, Å				
Ni–N	1.906(2)	1.902(2)	1.914(9)	1.916(12)	1.903(1)	1.952(4)	
N–Cα	1.381(2)	1.385(2)	1.395(4)	1.39(2)	1.387(12)	1.385(5)	1.379(6)
Cα–Cβ	1.451(3)	1.450(1)	1.455(6)	1.44(2)	1.444(3)	1.444(5)	1.443(5)
Cβ–Cβ	1.365(5)	1.360(2)	1.374(6)	1.36(2)	1.341(2)	1.332(8)	1.354(10)
Cα–Cm	1.395(2)	1.394(2)	1.387(4)	1.38(2)	1.384(2)	1.363(5)	1.390(11)
Cm–Cphen	1.491(1)	1.493(3)	1.488(6)	1.50(2)	1.494(3)		1.499(5)
Ct–N	1.906(3)	1.901(2)	1.914(5)	1.916(12)	1.903(2)	1.952(4)	
Ct–Cα	2.927(4)	2.923(2)	2.956(5)	2.94	2.930(2)	3.009(3)	
Ct–Cm	3.346(5)	3.338(1)	3.371(4)	3.35	3.344(2)	3.382(1)	
Ct–Ct	8.02	8.90	9.88	8.64	7.31	4.80	
o phen–Cβ	3.40(2)	3.38(2)	3.40(2)	3.52	3.42(2)		
o phen–Cβ subs't	3.36(2)	3.34(2)	3.33(3)				
			Bond Angles, deg				
Ni–Ni–N(adj)	90.6(2)	90.6(1)	90.5(1)	90.6(5)	90.6(1)	90.0(2)	
Ni–Ni–N(opp)	168.7(1)	168.6(1)	169.7(5)	168.4(5)	168.4(2)	180.0	
Cα–N–Cα	105.9(2)	105.8(1)	105.6(5)	108(1)	106.7(2)	104.1(4)	105.5(3)
Cα–Cβ–Cβ	106.8(1)	107.0(1)	107.0(4)	108(1)	107.8(1)	107.2(3)	107.0(1)
Ni–N–Cα	125.3(2)	125.0(2)	125.9(4)	125	125.2(2)	128.0(4)	
N–Cα–Cβ	109.8(1)	109.5(1)	110.0(2)	108(1)	108.4(1)	110.8(4)	110.2(2)
Cα–Cm–Cα	121.4(1)	121.5(2)	121.8(5)	122	121.5(3)	125.2(5)	123.8(3)
N–Cα–Cm	121.3(2)	120.8(1)	122.3(3)	123(1)	121.9(3)	124.4(4)	125.7(2)
Cβ–Cα–Cm	128.3(1)	129.1(1)	127.1(3)	128	129.0(2)	124.8(2)	124.2(1)
phen–porp	43(1)	39(3)	50(2)	58.3(6)	44.8(18)		

[a] The esd of the mean was calculated as $[\sum m(1_m - \bar{1})^2/m(m-1)]^{1/2}$ for more than two contributors and as the average of the esds for two contributors. [b] 2,3,7,8,12,13,17,18-Octabromo-5,10,15,20-tetramesitylporphyrin, saddle.[17] [c] 2,3,7,8,12,13,17,18-Octabromo-5,10,15,20-tetrakis(pentafluorophenyl)porphyrin, saddle.[18] [d] 2,3,7,8,12,13,17,18-Octaethylporphyrin, planar, Brennan et al.[4] [e] Hoard average of 16 porphyrins.[28]

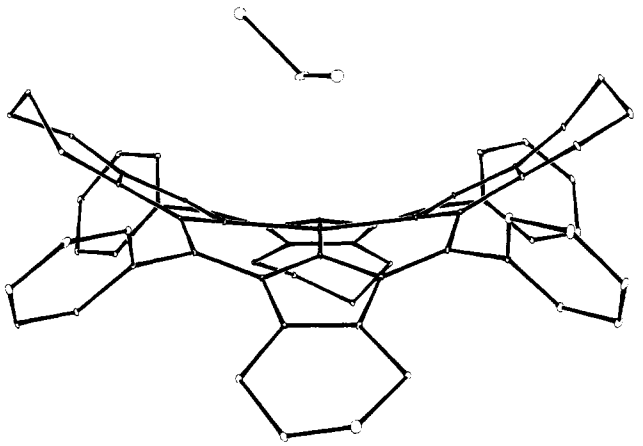

Figure 5. Edge-on-view of **3** and of the CH_2Cl_2 molecule of solvation.

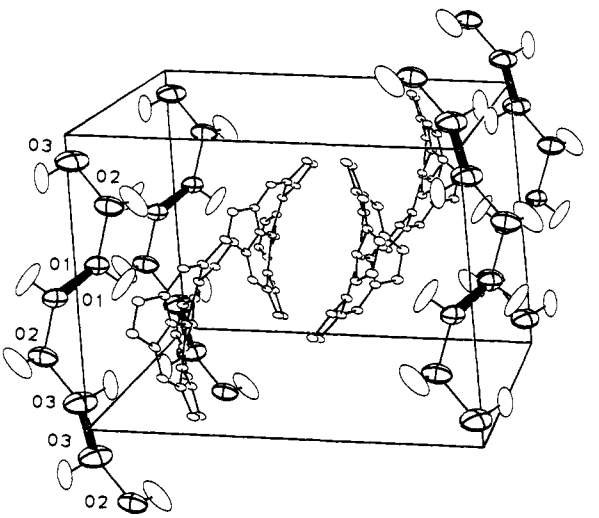

Figure 6. Packing diagram of **1** and of its methanols of solvation. The cross-hatched ellipsoids represent the oxygen atoms, and the adjacent atoms are the carbons of the methanols. The lines connecting the oxygens indicate the OH–O bonds. The heavy lines mark the beginning of a new set of three methanols associated with each porphyrin.

We present here solution and powder EXAFS data for **1**, **2**, and **3** and extend the studies to **4**, **5**, and **6**. The poor solubility of **5** in common solvents restricted that study to amorphous samples only. The near-edge features of **1**–**4** and **6** in solution exhibit the peaks diagnostic of square planar Ni(II), Figure 7. The compounds thus retain a tetracoordinate low-spin Ni(II) geometry in solution. The amorphous samples of **1**–**6** are tetracoordinate as well. (Data are included in the supplementary material.)

Analysis of the EXAFS data for **1**–**6** yields the average Ni–N distances shown in Table III. (Calculated fits for **2**, **5**, and **6** are shown in Figure 8. Data and analyses for the other compounds are included in the supplementary material.) Comparisons of the EXAFS results with the available crystallographic data and molecular mechanics calculations[11b,12c] are presented in Table III. The solution Ni–N distances of **1**–**3** agree well with the crystallographic results, within the precision of the EXAFS data, 0.02 Å. The short Ni–N distances establish that the nonplanarity of **1**–**3** is *maintained* in solution and thus is an inherent property of the crowded macrocycles. Likewise, the very short Ni–N distances of 1.88 Å in **4** suggest a very distorted conformation for NiDPP in solution, in agreement with the X-ray structure of H_2DPP which reveals a saddle conformation.[12b] In contrast, the long Ni–N distances of 1.97 Å in amorphous samples of **5** clearly signal a planar structure, as previously predicted by molecular mechanics calculations.[11b] (To ensure the reliability of the data on amorphous samples, data were also collected on amorphous **1**–**4**. Within the precision of the EXAFS measurements, the Ni–N values in the powder samples are similar to those found in solution, see Table III).

5 has not been crystallized to date. Crystals of the more soluble **6** have been obtained and their structure determined. Unlike **1**–**3**, **6** adapts a *ruf* conformation,[27] again with short Ni–N distances of 1.917(4) Å.[12c] However, the Ni–N distances determined by EXAFS are 1.96 Å in solution, 1.97 Å in the powder at room temperature, and 1.96 Å in a glass at 110 K, clearly indicative of a planar conformation. The planar con-

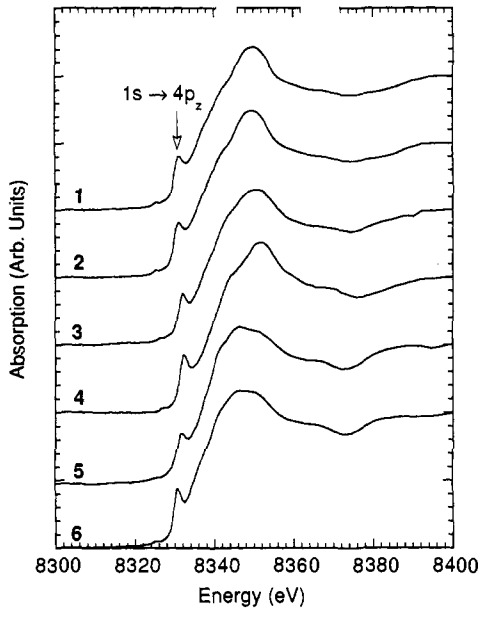

Figure 7. X-ray absorption near-edge spectra of **1–4** and **6** in toluene and of amorphous **5**. Note the preedge 1s → 4p$_z$ peaks characteristic of tetracoordinate Ni(II). T = 298 K.

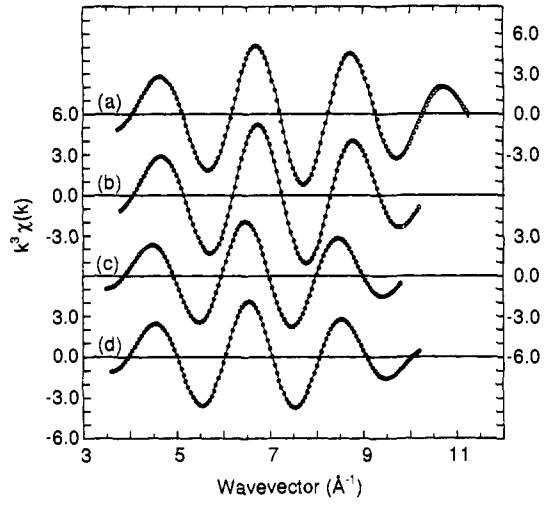

Figure 8. Isolated first-shell EXAFS oscillations (—) and nonlinear least-squares fits (O) for (a) amorphous **2**, 4 N at 1.92 Å, (b) **2** in toluene, 4 N at 1.91 Å, (c) amorphous **5**, 4 N at 1.97 Å, and (d) **6** in toluene, 4 N at 1.96 Å. T = 298 K.

formation is also predicted by molecular mechanics calculations with Ni–N values of 1.97 Å[12c] and is consistent with both NMR and resonance Raman results.[12c] Furthermore, the X-ray structure of the Cu(II) analog of **6** reveals a planar conformation with maximum deviations from the plane of the four nitrogens of 0.06 Å at the β pyrrole carbons and 0.09 Å at the meso carbons.[12c] In contrast to **1–4**, the macrocycle of **6** is thus *not* inherently distorted, and the ruffling of **6** must be due to crystal packing forces. Indeed, the CβCβCH$_2$ angles in **6** average 112.0(6)°[12c] to be compared with values of 125.5(1), 126.0(1), and 123.0(4)° in **1**, **2**, and **3**, respectively. The cyclopentenyl rings of **6** (and **5**) must therefore be small enough so as not to cause steric crowding between the β substituents and the aryl rings. In agreement with this suggestion, the dihedral angles of the aryl rings with the porphyrin planes are 64° in **6**[12c] but range between 39 and 50° in **1–3**.

Additional evidence of the skeletal flexibility of **6** derives from the observation that the low-spin Ni(II) complex can be converted to a hexacoordinated high-spin species. Previous EXAFS studies of Ni(II) porphyrins and hydroporphyrins[14] have established that the change to the high-spin states induces a lengthening of the Ni–N distances *and* requires that the macrocycles be flexible enough to accommodate the change to a planar conformation. At room temperature in pure pyridine, **6** exists as a mixture of tetra- and hexacoordinated species with Soret maxima at 411 and 432 nm, respectively. Upon lowering the temperature to ~245 K, the compound is converted to the hexacoordinated high-spin form with a maximum at 432 nm, a Soret shift comparable to those observed in NiOEP,[11b] NiTPP,[11b] and the parent NiT(OMeP)P, **7**. (The Soret peak of the latter shifts from 418 nm in butyronitrile or CH_2Cl_2 to 438 nm in pyridine at 245 K upon conversion to high spin Ni(II)). In contrast, the Soret bands of **1–4** show no evidence of coordination with pyridine[11b] nor any temperature dependence in accord with restricted conformations. (Optical data are included in the supplementary material.)

The combination of crystallographic, EXAFS, and ligation studies thus clearly establishes that **1–4** maintain their saddle conformation in solution and in the amorphous state and that their nonplanarity is induced by steric crowding between substituents. The cyclopentenyl substituents of **5** and **6**, on the other hand, apparently do not result in steric crowding, and the compounds are planar in solution (**6**) or in the amorphous state (**5** and **6**). As is evident from Table III, the experimentally observed Ni–N distances agree well with molecular mechanics predictions.[11b,12c]

Optical Spectra and Redox Potentials. A general consequence of the macrocycle distortions is that the optical transitions of the compounds are red-shifted compared to more planar molecules[9-12] (Table IV). INDO/s calculations[9] suggest that the effect is due to the destabilization of the porphyrin π system and that the gap between the HOMOs and LUMOs is smaller, resulting in red-shifts of the optical spectra. INDO/s calculations of the low-energy optical bands of **1**, **2**, and **3**, based on the crystallographic coordinates reported here, agree well with the experimental results, Table IV. The theoretical calculations thus reinforce the conclusions reached above that the saddle conformations are retained in solution. (For comparison, the calculated value for the planar NiOEP[4] agrees within better than 4% with the experimental result.) Note also that the first optical transition of **6**, which is deduced to be planar in solution on the basis of the EXAFS results, is not significantly shifted from those of NiOEP, NiTPP, or NiT(OMeP)P.

The experimental redox potentials for **1–4** and **6**, determined by cyclic voltammetry, are presented in Table IV. The redox potentials of porphyrins track the energy levels of the HOMOs and LUMOs of the complexes, and the differences between the first oxidation and reduction potentials, neglecting solvation effects, provide an indication of the energy of the first absorption band of porphyrins since this transition is principally a HOMO to LUMO excitation.[15,16,29]

The differences between the half wave potentials, ΔE, listed in Table IV, agree reasonably well with the energies of the first optical transitions (the maximum deviation between the redox and optical data is <8%), and thus support the notion that the redox potentials reflect the relative energies of the HOMOs and LUMOs in both planar and nonplanar macrocycles.

The oxidation and reduction potentials of **1**, **2**, and **3** fall within a narrow range, not surprisingly, since small differences due to the different substituents may be canceled by the slightly different saddle conformations of the three compounds. Typically, porphyrins with β alkyl substituents such as OEPs are easier to oxidize and harder to reduce than porphyrins with meso phenyl substituents.[29] Although **1**, **2**, and **3** are basically hybrids of the two major types of substitutions, the three compounds are easier to oxidize that either NiOEP or NiTPP, Table IV, in agreement with the theoretically predicted destabilization of the π systems

(29) Felton, R. H. In *The Porphyrins*; Dolphin, D., Ed.; Academic Press: New York; Vol. 5, p 53.

Table III. Summary of EXAFS, Crystallographic, and Molecular Mechanics Results

compd	Ni–N(calcd),[a] Å	Ni–N(cryst),[b] Å	Ni–N(EXAFS),[c] Å	form[d]	N[e]	$\Delta\sigma^2$[f]	χ^2_{gof}[g]
1	1.90	1.906(2)	1.90	toluene	4.50[h]	0.004	0.118
			1.91	tetrahydrofuran[i]	3.57	0.001	0.002
			1.93	powder	4.05	0.003	0.006
2	1.90	1.902(2)	1.91	toluene	3.52	–0.001	0.004
			1.92	powder	3.96	0.001	0.017
3	1.93	1.914(9)	1.93	tetrahydrofuran[i]	3.93	0.004	0.004
			1.91	powder	3.60[h]	0.003	0.030
4	1.91		1.88	toluene	3.80[h]	0.000	0.157
			1.91	powder	3.70[h]	0.003	0.014
5	1.97		1.97	powder	3.98	0.003	0.003
6	1.97	1.917(4)[12c]	1.96	toluene	3.64	0.003	0.001
			1.96	toluene glass, T = 110 K	3.95	0.002	0.041
			1.97	powder	3.70[h]	0.004	0.028

[a] Molecular mechanics calculations.[12a,c] [b] Crystallographic results. [c] Estimated precision: 0.02 Å. Typical analysis parameters: k^3 weighting, k = 3.6–10.4 Å^{-1}, r = 1.0–2.0 Å, ΔE_0 = –2 eV. Additional experimental details are included in the supplementary material. [d] Toluene solutions and amorphous powders at 298 K, unless otherwise specified. [e] Coordination number. [f] Relative mean square deviation in r (the square of the Debye–Waller factor). $\Delta\sigma^2 = \sigma^2_{unknown} - \sigma^2_{standard}$ (α^2 = 0.001). [g] $\sum$(experimental – fit)$^2/\sum$experiment.[2] [h] Fixed value for N. [i] Compound is more soluble in THF than in toluene. The near-edge feature characteristic of tetracoordinated Ni is also observed in THF.

Table IV. Optical Transitions and Redox Potentials

compound	λ calcd,[a] nm	λ obsd,[b] nm	E_{opt},[c] eV	$\Delta E_{1/2}$,[d] V	$E_{1/2}$(ox),[e] V	$E_{1/2}$(red),[e] V
NiOEP	570	550	2.25	2.29	0.92	–1.37
NiTPP		558	2.22	2.31	1.15	–1.16
NiOETPP (**1**)	587	588	2.11	2.26	0.85	–1.41
NiOPrTPP (**2**)	589	589	2.11	2.27	0.83	–1.44
NiTC$_6$TPP (**3**)	588	580	2.14	2.24	0.84	–1.40
NiDPP (**4**)		614	2.02	2.04	0.87	–1.17
NiTC$_5$T(OMeP)P (**6**)		554	2.24	2.21	0.96	–1.25
NiT(OMeP)P (**7**)		548	2.26	2.30	1.14	–1.16

[a] INDO calculations of the first optical transition, based on the crystallographic coordinates reported here for **1–3** and those for planar NiOEP by Brennan et al.[4] [b] Wavelength of the first optical transition, measured in butyronitrile. [c] Energy of the first optical transition in butyronitrile (1240 nm = 1 eV). [d] $E_{1/2}$(ox) – $E_{1/2}$(red) in butyronitrile. [e] Half-wave potentials in butyronitrile with 0.1 M Bu_4NClO_4 vs SCE.

due to the saddle conformations. This trend is also observed in the saddle-shaped ZnOETPP when compared to ZnOEP and ZnTPP.[9] The reduction potentials of **1**, **2**, and **3** are closer to those of NiOEP and again follow the trend observed in ZnOETPP[9] that the LUMO into which the electron is added is less sensitive to the conformations than the HOMO resulting in a smaller gap between the two and causing the optical red-shifts.[9] Comparison of potentials in **4** is complicated by the lack of experimental results for β substituted aryl models, but the molecule is again easier to oxidize than NiTPP while the reduction potential is equivalent to that of NiTPP.

In contrast to the shifts of 0.30 and 0.25 V in the oxidation and reduction potentials, respectively, of the saddle-shaped **1** relative to its parent component NiTPP, planar **6** is easier to oxidize by 0.18 V and harder to reduce by only 0.09 V than its parent NiT(OMeP)P, **7**. These effects may simply be due to the β alkyl substituents since NiOEP is easier to oxidize and harder to reduce than NiTPP, see Table IV.

Concluding Remarks

We have sought to assess here the influence of different β substituents on the conformations of a series of Ni(II) tetraphenyl derivatives. Crystallographic results establish that ethyl, propyl, and cyclohexenyl substitutions lead to saddle conformations of the macrocycle skeletons that minimize steric interactions between the β and meso substituents. We have also taken advantage of the sensitivity of Ni–N distances to the planarity or ruffling of Ni porphyrins to establish that the saddle distortions of **1**, **2**, and **3** are maintained in solution. The Ni–N distances in solution agree well with the crystallographic values, within the precision of the EXAFS measurements, 0.02 Å. The EXAFS results also establish that NiDPP, **4**, is very distorted in solution. Although a structure of **4** has not been determined, the results are consistent with the crystallographic saddle structure of the free base analog, H_2DPP.[12b] In contrast to these results, the EXAFS data for amorphous samples of NiTC$_5$TPP (**5**) are only consonant with a planar conformation, as predicted by molecular mechanics calculations.[11b] As well, EXAFS results also signal a planar conformation in solution for the more soluble trimethoxyphenyl derivative, **6**. Although the latter results would appear to contradict the *ruf* conformation of crystalline **6**,[12c] the planar conformation in solution is consistent with its NMR and optical spectra and molecular mechanics calculations.[12c] That the macrocycle of **6** is not sterically constrained is also evident from the fact that it will bind nitrogenous ligands to form the hexacoordinated high-spin Ni(II), unlike **1**, **2**, **3**, and **4**, and that the crystal structure of the Cu(II) complex of **6** shows the macrocycle to be planar.[12c] The different conformations of the cyclopentenyl derivatives thus point to the high sensitivity of the skeletal distortions to steric interactions between β and meso substituents.

The present results, previous crystallographic determinations,[2-19] and ongoing studies unambiguously establish that the skeletons of porphyrins and hydroporphyrins are highly flexible in vitro and in vivo. An increasing body of information[9-18] documents the significant effects that such conformational variations can have on optical, redox, NMR, EPR, vibrational, and excited-state properties of the molecules and reinforces the premise that such variations offer an attractively simple mechanism for modulating the physical and chemical properties of porphyrin chromophores and prosthetic groups in vitro and in vivo.[9] In this context, we note that an extensive series of OETPP derivatives that includes the free base, the diacid salt, and the Zn, Cu, Co, Fe, and Ni derivatives has been synthesized, and their structures (except for the Fe) have been determined as having saddle conformations.[9-12,30] This series thus affords the potential of determining the effects of the skeletal distortions on the chemistry of the metals and macrocycles and further allows comparison of these effects with the extensive data base that exists for OEPs and TPPs. The general good agreements between experimental results and molecular orbital[9,10,12a,15] and mechanics calcula-

(30) Unpublished results.

tions[11,12,15,31] further proffer the promise that such calculations can correctly predict the conformations and properties of existing and yet-to-be synthesized porphyrins of interest in photosynthesis, catalysis, photodynamic therapy, and electron transfer.[16]

Acknowledgment. We thank J. A. Shelnutt for useful discussions and the authors of refs 12 and 18 for communicating their results prior to publication. This work was supported by the Division of Chemical Sciences, U.S. Department of Energy, under Contract DE-AC02-76CH00016 at Brookhaven National Laboratory, and by National Science Foundation Grant CHE-90-01381 at the University of California. X-ray absorption data were collected on beam lines X11A and X19 of the National Synchrotron Light Source at BNL. X11A is supported by the Division of Materials Sciences, U.S. Department of Energy, under Contract DE-FG05-89ER45384. C.J.M. gratefully acknowledges a Fulbright Travel Scholarship and an Associated Western Universities Postdoctoral Fellowship.

(31) Munro, O. Q.; Bradley, J. C.; Hancock, R. D.; Marques, H. M.; Marsicano, F.; Wade, P. W. *J. Am. Chem. Soc.* **1992**, *114*, 7218.

Supplementary Material Available: Final positional and thermal parameters for the non-hydrogen atoms of **1–3** at 200 K and for **2** at 298 K, X-ray absorption data and experimental details for **1–4** and **6** in solution and for **1–6** as amorphous powders (k^3 weighted EXAFS data, Fourier transforms, isolated first-shell EXAFS and nonlinear least squares fits, and near edge data for amorphous samples of **1–6**), optical data for **6** in CH_2Cl_2 and pyridine and for **1–4** and **7** in pyridine at 298 and 245 K (48 pages); tables of calculated and observed structure factors for **1–3** (114 pages). Ordering information is given on any current masthead page.